Human blood vessel organoids recapitulate key mechanisms of transition from vasculopathy to fibrosis in systemic sclerosis

Yanhua Xiao, Xuezhi Hong, Langxian Zhi, Yi-Nan Li, Martin Regensburger, Franz Marxreiter, Boris Görg, Sarah Koziel, Andrea-Hermina Györfi, Tim Filla, Peter-Martin Bruch, Philipp Tripal, James Adjaye, Sascha Dietrich, Jürgen Winkler, Jörg H.W. Distler, Alexandru-Emil Matei

Article - Version of Record

Suggested Citation:
Xiao, Y., Hong, X., Zhi, L., Li, Y.-N., Regensburger, M., Marxreiter, F., Görg, B., Koziel, S., Györfi, A.-H., Filla, T., Bruch, P.-M., Tripal, P., Adjaye, J., Dietrich, S., Winkler, J., Distler, J., & Matei, A.-E. (2026). Human blood vessel organoids recapitulate key mechanisms of transition from vasculopathy to fibrosis in systemic sclerosis. Annals of the Rheumatic Diseases, 85(7), 1365–1380. https://doi.org/10.1016/j.ard.2026.02.021

Ann Rheum Dis 85 (2026) 1365–1380

Contents lists available at ScienceDirect

Annals of the Rheumatic Diseases

journal homepage: https://www.sciencedirect.com/journal/annals-of-the-rheumatic-diseases

Systemic sclerosis

Human blood vessel organoids recapitulate key mechanisms of transition from vasculopathy to fibrosis in systemic sclerosis

Yanhua Xiao[1,2,3,4,5], Xuezhi Hong[1,2,3,4,6], Langxian Zhi[1,2], Yi-Nan Li[1,2,7], Martin Regensburger[4,8,9,10], Franz Marxreiter[9,10], Boris Görg[11,12], Sarah Koziel[7,13,14,15,16], Andrea-Hermina Györfi[1,2,17,18], Tim Filla[1,2], Peter-Martin Bruch[7,13,14,15,19], Philipp Tripal[20], James Adjaye[21,22], Sascha Dietrich[7,13,14,15,19], Jürgen Winkler[9,10], Jörg H.W. Distler[1,2,7,17,18], Alexandru-Emil Matei[1,2,17,18,*]

[1] *Department of Rheumatology, University Hospital Düsseldorf, Medical Faculty of Heinrich Heine University, Düsseldorf, North Rhine-Westphalia, Germany*
[2] *Hiller Research Center, University Hospital Düsseldorf, Medical Faculty of Heinrich Heine University, Düsseldorf, North Rhine-Westphalia, Germany*
[3] *Department of Internal Medicine 3, Rheumatology and Clinical Immunology, Friedrich-Alexander-University Erlangen-Nürnberg (FAU) and University Hospital Erlangen, Erlangen, Bavaria, Germany*
[4] *Deutsches Zentrum Immuntherapie (DZI), University Hospital Erlangen, Kussmaullallee, Erlangen, Bavaria, Germany*
[5] *Department of Dermatology, The First Affiliated Hospital of Gannan Medical University, Gannan Medical University, Ganzhou, China*
[6] *Department of Rheumatology, The First Affiliated Hospital of Gannan Medical University, Gannan Medical University, Ganzhou, China*
[7] *Spatial and Functional Screening Core Facility, Medical Faculty of Heinrich Heine University, Düsseldorf, North Rhine-Westphalia, Germany*
[8] *Department of Stem Cell Biology, Friedrich-Alexander-Universität (FAU) Erlangen-Nürnberg, Erlangen, Bavaria, Germany*
[9] *Center for Rare Diseases Erlangen (ZSEER), University Hospital Erlangen, FAU Erlangen-Nürnberg, Erlangen, Bavaria, Germany*
[10] *Department of Molecular Neurology, FAU Erlangen-Nürnberg, Erlangen, Bavaria, Germany*
[11] *Clinic for Gastroenterology, Hepatology, and Infectiology, Heinrich Heine University, Düsseldorf, North Rhine-Westphalia, Germany*
[12] *Advanced Light Microscopy Core Facility (Ad-Light), Medical Faculty of the Heinrich Heine University, Düsseldorf, North Rhine-Westphalia, Germany*
[13] *Department of Haematology, Oncology and Clinical Immunology, University Hospital Düsseldorf, Düsseldorf, North Rhine-Westphalia, Germany*
[14] *Center for Integrated Oncology Aachen-Bonn-Cologne-Düsseldorf, Aachen, Bonn, Cologne, North Rhine-Westphalia, Germany*
[15] *Molecular Medicine Partnership Unit, Heidelberg, Baden-Württemberg, Germany*
[16] *Düsseldorf School of Oncology, Düsseldorf, North Rhine-Westphalia, Germany*
[17] *Fraunhofer Institute for Translational Medicine and Pharmacology ITMP, Frankfurt am Main, Hesse (Hessen), Germany*
[18] *Fraunhofer Cluster of Excellence for Immune Mediated Diseases CIMD, Frankfurt am Main, Hesse (Hessen), Germany*
[19] *Department of Hematology, Oncology and Rheumatology, University Hospital Heidelberg, Heidelberg, Germany*
[20] *Optical Imaging Competence Centre, Friedrich-Alexander-Universität Erlangen-Nürnberg, Erlangen, Bavaria, Germany*

*Correspondence to Dr Alexandru-Emil Matei, Department of Rheumatology and Hiller Research Center, University Hospital Düsseldorf, Heinrich Heine University, Düsseldorf, Germany.
E-mail address: alexandru-emil.matei@med.uni-duesseldorf.de (A.-E. Matei).
Xuezhi Hong and Yanhua Xiao contributed equally and share first authorship.
Handling editor Josef S. Smolen.

https://doi.org/10.1016/j.ard.2026.02.021

[21] *Institute for Stem Cell Research and Regenerative Medicine, University Hospital Düsseldorf, Duesseldorf, North Rhine-Westphalia, Germany*
[22] *Zayed Centre for Research into Rare Diseases in Children (ZCR), University College London (UCL)-EGA Institute for Women's Health, London, UK*

ARTICLE INFO

Article history:
Received 26 July 2025
Received in revised form 3 February 2026
Accepted 22 February 2026

ABSTRACT

Objectives: Systemic sclerosis (SSc) is an autoimmune disease that transitions from vasculopathy as an initiating pathogenic event to tissue fibrosis. The mechanisms of these transitions remain, however, poorly understood, mainly because complex multicellular human models of SSc vasculopathy are lacking. We aimed to develop a complex multicellular human model of SSc vasculopathy and use it to investigate the mechanisms underlying this process.

Methods: Blood vessel organoids (BVOs) were derived from induced pluripotent stem cells of patients with SSc and healthy controls. Organoids were exposed to serum from patients with SSc with clinically manifest microvasculopathy or healthy donors. Structural and molecular changes were evaluated using confocal imaging, transcriptomic (RNA sequencing), epigenetic (assay for transposase-accessible chromatin sequencing), and spatial proteomic (codetection by indexing) profiling. Serum immunoglobulin G (IgG) was selectively depleted or enriched to investigate antibody contributions. Therapeutic interventions included bosentan and the γ-secretase inhibitor N-[N-(3,5-difluorophenacetyl)-L-alanyl]-S-phenylglycine t-butyl ester (DAPT).

Results: SSc-derived BVOs exposed to SSc serum exhibited profound angiogenic defects, characterised by reduced vessel integrity, loss of endothelial-pericyte interactions, and induction of endothelial-to-mesenchymal transition (EndMT). Epigenetic and transcriptional profiling revealed upregulation of fibrosis-related genes and loss of endothelial markers. Spatial proteomic data confirmed EndMT at the protein level and demonstrated shifts in endothelial and pericyte subpopulation as well as alterations in their interactions reminiscent of those seen in tissues of patient with SSc. IgG depletion from SSc serum restored vascular structure, and transfer of SSc IgG to healthy serum phenocopied the pathological phenotype, implicating autoantibodies in endothelial injury. Both bosentan and DAPT partially reversed vascular abnormalities and downregulated EndMT markers.

Conclusions: This study establishes BVOs as a complex human model of SSc vasculopathy and demonstrates in a multiomic approach that they recapitulate disease-specific vascular dysfunction and its transition to fibrosis. We show that genetic susceptibility and pathogenic autoantibodies synergise in driving microvascular injury in SSc. Furthermore, we provide evidence that SSc BVOs are a promising platform for evaluating therapies that prevent the transition from vasculopathy to fibrosis, and present Notch/γ-secretase inhibition as a potential novel target in SSc vasculopathy.

INTRODUCTION

Connective tissue diseases, also known as collagen vascular diseases, are autoimmune disorders within the rheumatic spectrum, characterised by vasculopathy, inflammation, and tissue fibrosis as shared pathogenic features. Systemic sclerosis (SSc) is the connective tissue disease associated with the highest case-specific mortality of all autoimmune rheumatic diseases [1]. SSc is characterised by widespread vasculopathy, autoimmunity, and fibrosis [2,3]. Therapeutic options remain limited to date [4]. Microvasculopathy is the first detectable manifestation of SSc and is thought to be the initiating event that not only triggers autoimmunity and fibrosis, but also plays a crucial role in disease progression [5,6]. SSc is thus a prototypical connective tissue disease that transitions from microvasculopathy to inflammation and tissue fibrosis.

Endothelial cell (EC) damage triggers a cascade of pathologic events, including aggregation of platelets at the denuded basal membrane, recruitment of leukocytes, and subsequent activation of fibroblasts. Microvascular changes are visualised in the clinical routine by nailfold capillaroscopy. In the early stages of SSc, characteristic findings include capillary dilatation and distorted capillary architecture, whereas in advanced disease, these microvascular changes progress to loss of capillaries and small arteries, leading to avascular areas [7].

The vascular pathogenesis of SSc remains incompletely understood. EC dysfunction is thought to result from the interplay of inflammatory features such as autoantibodies and cytokines with a subsequent imbalance between proangiogenic and antiangiogenic factors in genetically predisposed individuals [8–10]. Several susceptibility genes have been implicated in endothelial damage and vascular pathology in SSc, including polymorphisms in genes related to angiogenesis or oxygen sensing [11–13]. However, the relative contribution of the individual drivers and their interplay remains elusive.

Our limited understanding of the vascular pathophysiology of SSc is at least in part a consequence of the paucity of preclinical models. Microvascular ECs are more challenging to isolate from fibrotic tissues of patients with SSc than many other cell types such as fibroblasts. Moreover, most mouse models of SSc do not recapitulate the microvascular features of SSc, and the few mouse models that display certain vascular features of SSc are difficult to breed and are available only at few centres [14]. Multicellular human *in vitro* models of the vascular changes in SSc with sufficient complexity have not been reported so far.

In this study, we aimed to assess whether blood vessel organoids (BVOs) derived from induced pluripotent stem cells (iPSCs) of patients with SSc and healthy individuals exposed to serum from patients with and without severe microvasculopathy can replicate key features of SSc vasculopathy. These BVOs are

WHAT IS ALREADY KNOWN ON THIS TOPIC

- Systemic sclerosis (SSc) is an autoimmune disorder in which microvasculopathy serves as the initiating pathogenic event, driving progression towards tissue fibrosis.
- Endothelial dysfunction and perturbed angiogenesis are recognised as hallmark features of vascular pathology in SSc.
- The mechanisms of transition from vasculopathy to fibrosis in SSc remain poorly understood, mainly due to the lack of human models that recapitulate the multicellular complexity and disease-specific vascular perturbations inherent to SSc.

WHAT THIS STUDY ADDS

- We established blood vessel organoids (BVOs) from patients with SSc as a complex human model that recapitulates endothelial cell and pericyte subpopulations, as well as endothelial-pericyte interactions and microvascular architecture.
- We demonstrate in a multiomic approach that these organoids recapitulate key features consistent with the pathological sequence seen in SSc, including early microvascular damage, endothelial-to-mesenchymal transition (EndMT), and vascular rarefaction when exposed to SSc serum from patients with clinically manifest microangiopathy.
- Both γ-secretase inhibition and treatment with bosentan restored endothelial homeostasis and attenuated aberrant EndMT, supporting the utility of the organoids as a platform for drug screening and demonstrating that Notch/γ-secretase might be a novel target in SSc.

HOW THIS STUDY MIGHT AFFECT RESEARCH, PRACTICE OR POLICY

- BVOs from SSc donors represent a unique human model that offers both sufficient complexity for studying cell-cell interactions that lead to vasculopathy and fibrosis, but also high throughput that allows drug screening.
- By recapitulating key pathologic mechanisms in SSc vasculopathy, BVOs from SSc donors bridge the gap between animal models and *in vitro* culture and enable scalable evaluation of candidate therapies for SSc and potentially other collagen vascular diseases.
- Pharmacological targeting of Notch/γ-secretase signalling may offer new strategies to preserve vascular function and limit fibrosis in early-stage SSc.

composed of ECs and pericytes (PEs), which self-assemble in 3-dimensional (3D) vessel structures. We conducted a comprehensive multiomics analysis to investigate how SSc-derived iPSCs and SSc serum induce an SSc-like vascular phenotype. Finally, we explored the potential of BVOs as a novel platform for testing vasoactive drugs for the treatment of SSc.

METHODS

Detailed descriptions of the materials and methods are available in the online supplementary materials due to word count limitations in the main text.

RESULTS

Generation of SSc and healthy BVOs and comparison of their vessel structure

We first generated BVOs from SSc-iPSCs and control-iPSCs (SSc-BVO and healthy BVO, respectively) following a previously described differentiation method [15,16]. The demographic and clinical characteristics of the iPSC donors are summarized in Supplementary Table S1. This involved reproducing vessel development in embryonal life, in several steps: (i) formation of aggregates from iPSC, (ii) mesoderm induction, (iii) vascular lineage induction with formation of vessel aggregates, and (iv) collection of single vascular networks and further vascular differentiation to form BVOs (Fig 1A). Confocal microscopy with an LSM 880 confocal microscope (Carl Zeiss, Jena, Germany) confirmed the successful formation of vascular networks in both groups, consisting of cluster of differentiation 31 $(CD31)^+$ ECs, platelet-derived growth factor receptor beta $(PDGFR\beta)^+$ and/or smooth muscle protein 22-alpha $(SM22)^+$ PEs, and a surrounding collagen type IV $(COLIV)^+$ basement membrane (Fig 1B,C, Supplementary Videos S1 and S2, Supplementary Fig S1A). 3D image reconstitution revealed intricate vascular structures in both healthy and SSc BVOs, where ECs formed tubular networks in close association with PEs and the basement membrane (Fig 1C, Supplementary Video S2).

We next analysed vessel morphology using 2 tools: (i) AngioTool [17], which relies on 2-dimensional maximum intensity projection representations of the 3D images, and (ii) VesselVio [18], which uses directly 3D images, to quantify vessel density, length, volume, and degree of branching, which are parameters commonly evaluated in nailfold capillaroscopy in clinical practice. SSc BVOs had a higher vessel density and total vessel length, thus indicating an upregulation of angiogenesis (Supplementary Fig S1B-G). However, the SSc BVOs also had a higher number of branching points and of vessel segments, as well as a higher average volume and a higher percentage of vessels with very high volume, indicating a lower degree of maturation of the newly formed vessels (Fig 1D-I). This reflects early changes in SSc vasculopathy, characterised by aberrant angiogenesis with the formation of highly branched immature vessels and the presence of giant capillaries [19,20].

Healthy male- and female-derived BVOs had comparable vessel length, density, and branching, suggesting that the gender-related effects on angiogenesis in BVOs are minimal (Supplementary Fig S2).

Exposure to serum from patients with SSc with severe vasculopathy induces angiogenic defects in SSc-BVOs

Although aberrant angiogenesis with the formation of immature vessels is typical for early stages of SSc, later disease stages are marked by angiogenic defects with extensive loss of small vessels [21]. We reasoned that circulating factors in patients with SSc might be required to reproduce this phenotype in SSc BVO. To test this hypothesis, we exposed SSc and healthy BVOs to serum from patients with SSc suffering from active ischaemic digital ulcers (current open ulcers with tissue loss present at the time of serum collection, excluding pitting scars/healed lesions and minor fissures/abrasions) as clinical manifestation of severe ongoing microangiopathy at the time of serum collection (denoted as serum from patients with SSc with active digital ulcers [SSc_aDU] serum) and serum from healthy donors (denoted as healthy serum) for 7 days. Exposure to serum from patients SSc without active digital ulcers (denoted as serum from patients with SSc without active digital ulcers [SSc_noDU] serum) was included to control for the effects of other disease-associated mediators (eg, proinflammatory and profibrotic) on angiogenesis. Systemic disease activity (European Scleroderma Trials and Research group (EUSTAR) activity index) was recorded for SSc serum donors and was predominantly high in both SSc_aDU and SSc_noDU groups, reducing the likelihood that differences were driven solely by

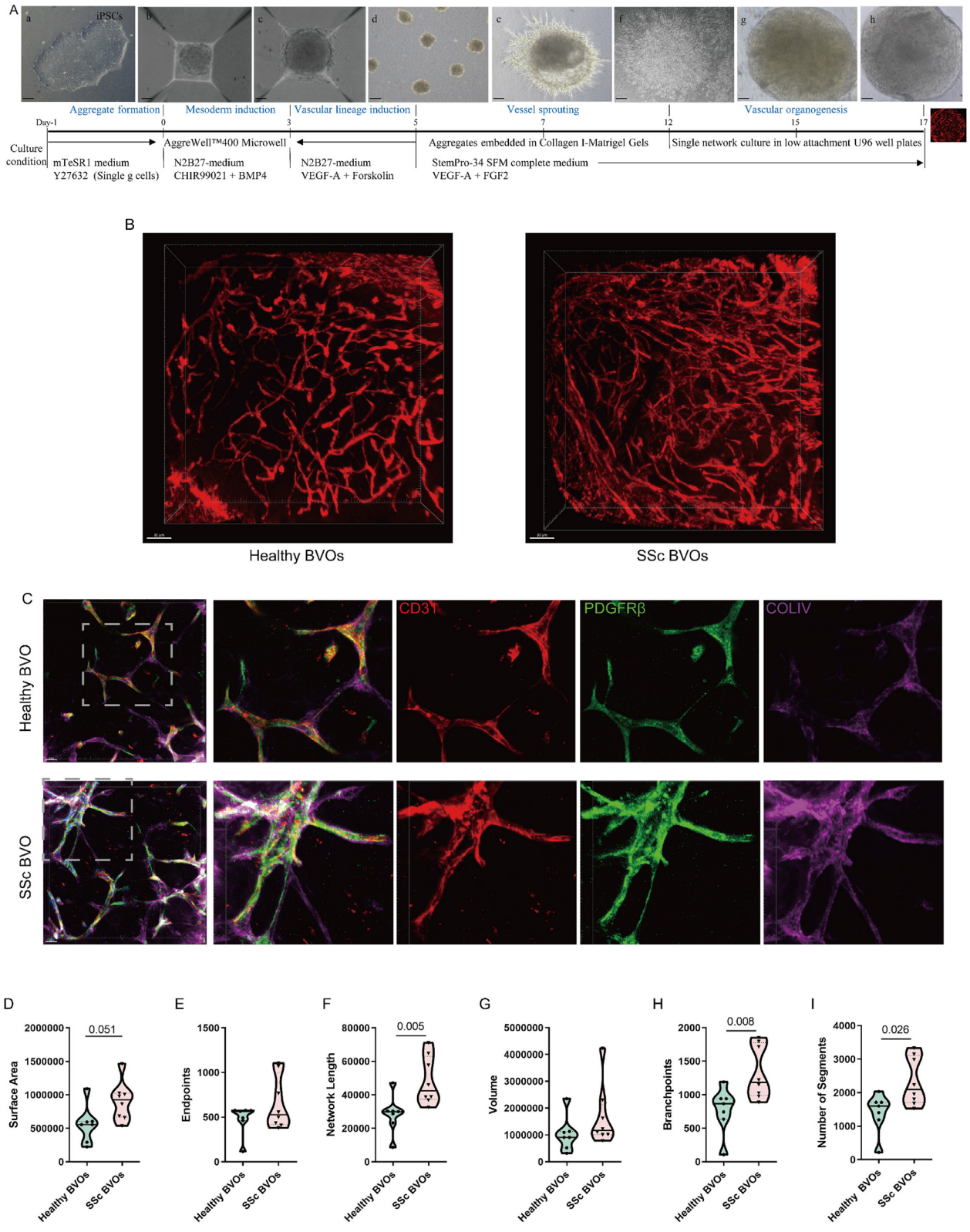

Figure 1. Generation and characterisation of BVOs derived from healthy and SSc-iPSCs. (A) Schematic representation of the protocol used for the differentiation of human pluripotent stem cells into BVOs. Representative phase contrast images at different timepoints during differentiation are included. Scale bars: 100 μm. (B) 3D rendering of confocal images of healthy and SSc-derived BVOs. CD31 immunostaining (red) identifies endothelial cells forming tubular vascular structures. Scale bars: 80 μm. (C) Confocal immunofluorescence of vascular networks in healthy and SSc BVOs, showing endothelial cells (CD31$^+$, red), pericytes (PDGFRβ^+, green), and basement membrane (COLIV$^+$, purple) (maximum intensity projection). Scale bars: 30 μm. (D-I) Quantitative comparison of vascular parameters between healthy and SSc BVOs, including surface area (D), endpoints (E), network length (F), volume (G), branchpoints (H), and number of segments (I), analysed using VesselVio [18] and ImageJ (National Institutes of Health, Bethesda, MD, USA), and shown as violin plots. Data points represent individual organoids. Healthy BVOs: 2 donors; 4 iPSC clones. SSc BVOs: 1 donor; 2 iPSC clones, with 1 to 5 organoids per clone. Statistically significant P values (Mann–Whitney U test) are included. BVO, blood vessel organoid; iPSC, induced pluripotent stem cell; SSc, systemic sclerosis; 3D, 3-dimensional; CHIR, CHIR99021; BMP4, bone morphogenetic protein 4; VEGF, vascular endothelial growth factor; SFM, serum-free medium; mTeSR1, mTeSR1 medium; PDGFR, platelet-derived growth factor receptor; COLIV, collagen IV; FGF2, fibroblast growth factor 2.

systemic inflammatory activity (Supplementary Table S2). Sera were pooled to reduce idiosyncratic single-donor effects (SSc_aDU serum n = 13; SSc_noDU serum n = 5; healthy serum n = 5).

We operationalised angiogenic defects as microvascular rarefaction of the vascular network in the BVOs, quantified by reduced vessel density/length/branching and reduced vascularised surface area/volume. SSc_aDU serum induced profound angiogenic defects in SSc BVOs, as evidenced by a reduction in vessel density, vessel length, number of junctions, branching index, surface area, and volume occupied by vessels (Fig 2A-G, Supplementary Fig S3A-F). In contrast, SSc_noDU serum caused only mild vascular changes (Fig 2A-G, Supplementary Fig S3A-F), suggesting that SSc BVOs can recapitulate the severity of vasculopathy of the serum donors. Interestingly, SSc_aDU serum induced only minor vasculopathic features in healthy BVOs (Fig 2A-G, Supplementary Fig S3A-F), which suggests that SSc BVOs are particularly vulnerable to SSc_aDU serum-induced vasculopathy. These findings highlight that the combination of genetic predisposition and serum-mediated effects is required to fully manifest SSc-associated microvascular changes in BVOs.

To evaluate possible associations of gene variants with the increased susceptibility of SSc BVOs for SSc_aDU serum-induced vasculopathy, we performed Sanger sequencing of the SSc and healthy iPSCs for 6 single-nucleotide polymorphisms (SNPs) that were previously linked to SSc susceptibility and/or to vasculopathy: (i) rs1799983 in nitric oxide synthase 3 (*NOS3*); (ii) rs1870377 in kinase insert domain receptor (*KDR*); (iii) rs2010963 in vascular endothelial growth factor A (*VEGFA*); (iv) rs5498 in intercellular adhesion molecule 1 (*ICAM1*); (v) rs4317244 in ankyrin repeat domain 37 (*ANKRD37*); and (vi) rs11217020 in DEAD-box helicase 6 (*DDX6*) (Supplementary Fig S4A-F, Supplementary Table S3) [12,22–25]. Both SSc donors carried the *VEGFA* rs2010963 GG genotype, whereas the 2 healthy donors carried the CC and CG genotype (Supplementary Fig S4C). The GG genotype was previously associated with impaired angiogenesis [26,27], and might, thus, contribute to the higher susceptibility of SSc BVOs to SSc_aDU serum.

Multiomics-based characterisation of SSc serum-induced vasculopathy in SSc BVOs

To characterise the mechanisms that lead to the profound angiogenic defects in SSc BVO exposed to SSc_aDU serum, we next performed a multiomics-based evaluation of SSc BVOs exposed to SSc_aDU and healthy serum at the epigenomic level by assay for transposase-accessible chromatin sequencing (ATACseq), at the transcriptomic level by RNA sequencing (RNAseq) and at a multiplexed protein level by codetection by indexing (CODEX).

Exposure to SSc_aDU serum induced both changes in chromatin accessibility and in transcriptomes of SSc BVOs, with 612 genes with differentially accessible regions (DARs) (104 with gain and 498 with loss of DAR), as well as 94 differentially expressed genes (24 upregulated and 70 downregulated) (Fig 3A,B).

Notably, several profibrotic genes, including actin alpha 2, smooth muscle (*ACTA2*), twist family bHLH transcription factor 1 (*TWIST1*), snail family transcriptional repressor 2 (*SNAI2*), transforming growth factor beta 2 (*TGFB2*), and collagen type I alpha 2 chain (*COL1A2*), gained DARs and were upregulated at the mRNA level in ECs purified from SSc BVOs, whereas several EC marker genes, such as claudin 5 (*CLDN5*), platelet and endothelial cell adhesion molecule 1 (*PECAM1*), cadherin 5 (*CDH5*), and von Willebrand factor (*VWF*), lost DARs and were downregulated at the mRNA level in ECs purified from SSc BVOs, suggesting a shift towards a profibrotic and endothelial-to-mesenchymal transition (EndMT)-like phenotype in SSc BVOs treated with SSc_aDU serum (Fig 3C,D). This EndMT-related gene expression shift induced by exposure to SSc_aDU serum was less consistent in ECs purified from healthy BVOs (Supplementary Fig S5A,B).

Pathway enrichment analysis revealed consistent de-enrichment of pathways related to tight junction, endothelial integrity, and vascular function, thus indicating a compromised endothelial phenotype, with enrichment of pathways related to collagen production, extracellular matrix organisation, contraction, transforming growth factor beta (TGF-β) and WNT signalling and leukocyte migration and activation in SSc BVOs exposed to SSc_aDU serum both at the epigenomic and at the transcriptomic level (Fig 3E,F, Supplementary Fig S5C,D). Furthermore, transcription factor (TF) activity inference from the RNAseq data provided evidence for decreased activity of TFs related to an EC phenotype, such as GATA binding protein 2 (*GATA2*), ETS proto-oncogene 1 transcription factor (*ETS1*), forkhead box O4 (*FOXO4*), nuclear factor of activated T cells 2 (*NFATC2*), ETS transcription factor 1 (*ELK1*), and ETS transcription factor 4 (*ELK4*) in ECs purified from SSc BVOs, and increased activity of profibrotic TFs, including AP-1 transcription factor subunit (*JUN*), RELA proto-oncogene, NF-κB subunit (*RELA*), SMAD family member 3 (*SMAD3*), and snail family transcriptional repressor 1 (*SNAI1*), in SSc BVOs exposed to SSc_aDU serum (Supplementary Fig S5E,F).

CODEX analysis confirmed that SSc_aDU serum induces angiogenic defects in SSc BVOs (Fig 3G,H) and demonstrated upregulation of EndMT markers (Twist1, zinc finger E-box binding homeobox 1 (ZEB1), SNAI1, and SNAI2), myofibroblast markers (αSMA), profibrotic TFs (FRA2), and increased expression of collagen type I at the protein level (Fig 3I-P; antibodies and manufacturer information are provided in Supplementary Table S4). Furthermore, SSc_aDU serum induces upregulation of ICAM1, an EC activation marker, in SSc BVOs (Fig 3O).

Of note, SSc_noDU serum treatment had milder pro-EndMT effects in SSc BVOs than SSc_aDU serum, and SSc_aDU serum had weaker and less consistent effects in inducing αSMA and EndMT markers in healthy BVOs (Fig 3I-P, Supplementary Fig S5G).

We further data mined a previously published single-cell RNAseq dataset from SSc and healthy skin (GSE138669 [28]), performed unbiased clustering and identified ECs based on their expression of specific genes such as *PECAM1, CDH5, VWF*, or ETS-related gene (*ERG*) (Supplementary Fig S6A-C). Differential expression analysis revealed that genes associated with EndMT, such as transforming growth factor beta 1 (*TGFB1*), collagen type IV alpha 1 chain (*COL4A1*), collagen type IV alpha 2 chain (*COL4A2*), and periostin (*POSTN*), along with the adhesion-related gene vascular cell adhesion molecule 1 (*VCAM1*), were upregulated in SSc ECs (Supplementary Fig S6D,E). Gene Ontology (GO) enrichment analysis of the genes upregulated in SSc indicated significant enrichment in pathways related to extracellular matrix organisation, TGF-β signalling, and cell adhesion (Supplementary Fig S6F). These analyses demonstrate that the transcriptomic changes induced by SSc_aDU serum in SSc BVOs recapitulate the transcriptomic changes in ECs from SSc skin.

Our multiomics approach, thus, highlights that exposure to SSc serum from patients with severe microvascular disease

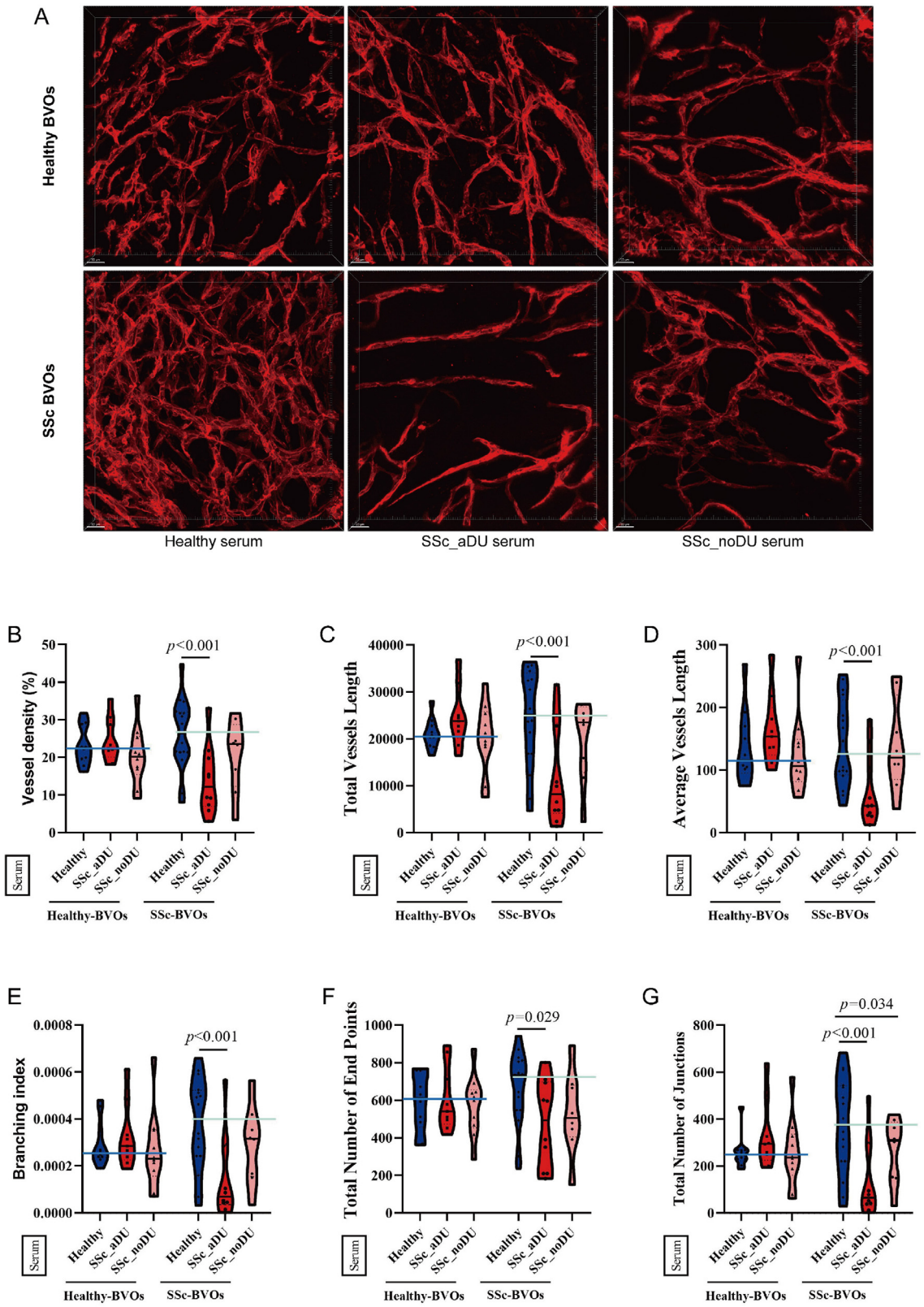

Figure 2. Serum from patients with clinically manifest microangiopathy induces angiogenic defects in SSc BVOs. (A) Representative 3D rendering of confocal images of healthy and SSc-derived BVOs treated with healthy serum, SSc_aDU serum, or SSc_noDU serum for 7 days. Active DU was defined as a current open digital ulcer with tissue loss present at the time of serum collection. Sera were pooled (healthy: n = 5 donors; SSc_aDU: n = 13 donors; SSc_noDU: n = 5 donors; see Supplementary Table S2). Endothelial cells forming vessel structures were identified by CD31 marker expression (red). Scale bars: 30 μm. (B-G) Quantitative analysis of vessel parameters using AngioTool, including vessel density (B), total vessel length (C), average vessel length (D), branching index (E), total number of endpoints (F), and total number of junctions (G), shown as violin plots. Each serum treatment condition included 4 different clones with 2 to 4 organoids each. *P* values are from LMMs with serum treatment as a fixed effect and a random intercept for iPSC clone, which accounts for the correlation of organoids derived from the same clone (avoiding pseudoreplication). BVO, blood vessel organoid; DU, digital ulcer; iPSC, induced pluripotent stem cell; LMM, linear mixed-effects model; SSc, systemic sclerosis; SSc_aDU serum, serum from patients with SSc with active digital ulcers; SSc_noDU serum, serum from patients with SSc without active digital ulcers; 3D, 3-dimensional.

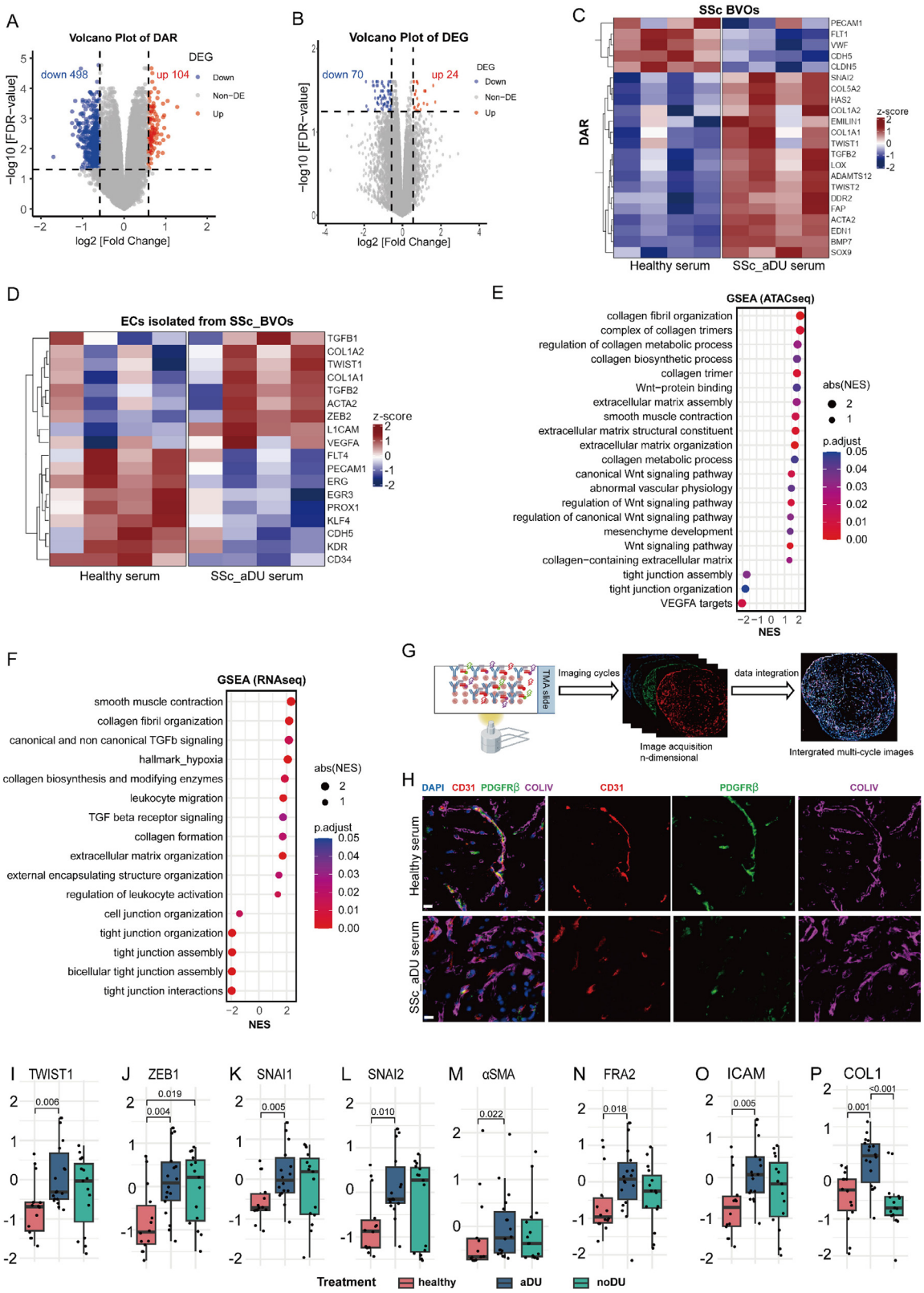

Figure 3. Multiomics-based characterisation of SSc serum-induced vasculopathy in SSc BVOs. (A) Volcano plot of ATACseq-based DARs in SSc BVOs exposed to SSc_aDU serum treatment compared with SSc BVOs exposed to healthy serum. Red and blue dots indicate genes with significantly upregulated and downregulated accessible regions, respectively (|log2 fold-change| > 0.585; FDR < 0.05). (B) Volcano plot of RNAseq-based DEGs between SSc BVOs treated with SSc_aDU serum and healthy serum. (C, D) Heatmap of EndMT-associated markers identified from ATACseq data of whole BVOs (C), and from RNAseq data of ECs isolated from SSc-BVOs (D), treated with SSc_aDU serum or healthy serum. (E) Bubble plot of GSEA based on ATACseq counts showing significantly enriched pathways in SSc BVOs treated with SSc_aDU serum compared with healthy serum. (F) Bubble plot of GSEA based on RNAseq counts between SSc_aDU serum and healthy serum-treated SSc BVOs. (G) Schematic illustration of multicycle imaging acquisition and data integration using CODEX technology. (H) Representative CODEX images of vascular structures of SSc BVOs treated with healthy serum or SSc_aDU serum. Markers include CD31 (red, endothelial marker), PDGFRβ (green, pericyte marker), and COLIV (magenta, basement membrane marker). Nuclei are stained with DAPI (blue). Scale bar, 20 µm. (I-P) CODEX-based protein expression levels of TWIST1 (I), ZEB1 (J), SNAI1 (K), SNAI2 (L), αSMA (M), FRA2 (N), ICAM (O), and COL1 (P) in SSc BVOs treated with healthy serum, SSc_aDU serum, or SSc_noDU serum (n ≥ 14

induces changes on the epigenetic, mRNA and protein levels to induce a vascular phenotype in SSc BVOs that reproduces key pathogenic features of SSc vasculopathy, including EndMT.

SSc BVOs recapitulate EC and PE populations observed in SSc skin

We next aimed to leverage the single-cell resolution of CODEX and evaluate changes in subpopulations of ECs and PEs and their function in SSc BVO upon treatment with SSc serum (Fig 4A). We analysed 70,660 cells, including 50,619 from SSc BVOs and 20,041 from healthy BVOs, each group exposed to either healthy, SSc_aDU or SSc_noDU serum.

We performed metaclustering of all cells to identify PEs, expressing high levels of PDGFRβ, regulator of G protein signalling 5 (RGS5), cluster of differentiation 90 (CD90), SM22, and αSMA, but no CD31; lymphatic ECs (LECs), expressing CD31 and high levels of lymphatic vessel endothelial hyaluronan receptor 1 (LYVE1), vascular endothelial growth factor receptor 2 (VEGFR2), and vascular endothelial growth factor receptor 3 (VEGFR3), and blood ECs (BECs), with strong expression of CD31, but with no or low levels of the PE- and LEC-specific markers (Supplementary Fig S7A,B).

We further aimed to evaluate whether SSc BVOs recapitulate BEC subpopulations identified in SSc skin by single-cell analyses in previous studies [28–30]. We subclustered the BECs and identified 8 distinct BEC subpopulations: (i) delta-like ligand 4 (DLL4)$^+$cluster of differentiation 34$^+$ BECs, with an endothelial tip cell phenotype; (ii) CD34$^+$ BECs; (iii) Hes-related family bHLH transcription factor with YRPW motif 1 (HEY1)$^+$DLL4$^+$CD34$^+$ BECs, demonstrating arterial BEC commitment; (iv) uclear receptor subfamily 2 group F member 2 (NR2F2)$^+$CD34$^+$ BECs, with venous BEC commitment; (v) tyrosine kinase with immunoglobulin-like and EGF-like domains 2 (TIE2)$^+$ BECs, with an endothelial stalk cell phenotype; (vi) endothelial progenitor cells (EPCs), expressing VEGFR2 and CD34, (vii) αSMA$^+$DLL4$^+$NR2F2$^+$ BECs, and (viii) aSMA$^+$NR2F2$^+$ BECs, expressing high levels of αSMA as a marker of EndMT (Fig 4B,D, Supplementary Fig S7C) [31]. Thus, BVOs reproduce key EC populations previously described in SSc and healthy vasculature, including arterial BECs, venous BECs, stalk and tip cell BECs, EPCs, αSMA$^+$ BECs, and LECs [28–30].

The 2 αSMA$^+$ EC populations expressed high levels of other EndMT-associated markers (SNAI1, SNAI2, ZEB1, and TWIST1) as well as high levels of intracellular collagen type 1, and are thus bona fide EC subsets undergoing EndMT (Fig 4C). Furthermore, they expressed high levels of the EC activation markers ICAM and VCAM, high levels of FRA2 and low levels of leukemia integration 1 transcription factor (FLI1) (Fig 4C), an expression pattern reminiscent of a dysfunctional EC phenotype previously described in SSc [32].

We further subclustered the PEs to evaluate whether SSc BVOs recover PE populations observed in SSc skin [29]. We identified 4 distinct populations: (i) CD90^{hi} PEs; (ii) aSMA-^{hi}SM22^{hi} PEs; (iii) PDGFRβ^{hi} PEs, and (iv) ADAM metallopeptidase domain 12 (ADAM12)^{hi} PEs (Supplementary Fig S8A,B). BVOs, thus, recapitulate previously described PE populations in SSc skin, including CD90^{hi}, PDGFRβ^{hi}, and ADAM12^{hi} PEs, as well as a population of aSMA^{hi}SM22^{hi} PEs that demonstrate evidence of PE-to-myofibroblast transition [29].

SSc BVOs exposed to SSc serum recapitulate shifts in frequencies of EC and PE populations observed in SSc skin

We further evaluated whether SSc_aDU serum induces shifts in frequencies of BEC and PE subsets in SSc BVOs. We observed remarkable shifts in BEC subpopulations following SSc_aDU serum treatment in SSc BVOs, with increases in frequencies of the 2 aSMA$^+$ populations that are undergoing EndMT and decreases in EC populations involved in angiogenesis (DLL4$^+$CD34$^+$ BECs, Tie2$^+$ BECs, and HEY1$^+$CD34$^+$DLL4$^+$ BECs) (Fig 4E-G). Of note, enrichment of an aSMA$^+$ subpopulation of ECs undergoing EndMT was previously described in SSc skin [29].

We further observed an increase in the frequency of the αSMA^{hi}SM22^{hi} and ADAM12^{hi} PEs and a decrease in the frequency of PDGFRβ^{hi} and CD90^{hi} PEs upon exposure of SSc BVOs to SSc_aDU serum (Supplementary Fig S8B,C). Enrichment of ADAM12^{hi} and αSMA^{hi} PEs, as well as loss of CD90^{hi} PEs, was previously described in SSc skin [29].

Taken together, these results demonstrate that exposure of SSc BVO to SSc_aDU serum reproduces shifts in EC and PE subsets observed in SSc skin.

Of note, the shifts in EC and PE subpopulations in response to SSc_aDU serum are weaker in healthy than in SSc BVOs (Supplementary Figs S7D and S8D).

Altered interaction networks of EC subsets with PEs in SSc BVOs exposed to SSc serum

Since ECs-PEs interactions are critical for physiological vessel development and maturation [33,34], we wondered whether these interactions might be impaired by exposure of SSc BVOs to SSc_aDU serum. To evaluate this, we leveraged the spatial resolution of CODEX to examine the changes in spatial proximity between BEC subpopulations and PEs in SSc BVOs exposed to serum from different donor groups (Fig 5A). On exposure to healthy serum, PEs were in close spatial proximity to multiple BEC subpopulations, including TIE2$^+$ BECs, HEY1$^+$CD34$^+$DLL4$^+$ BECs, and NR2F2$^+$CD34$^+$ BECs (Fig 5A,B). However, in SSc BVOs exposed to SSc_aDU serum, the interaction patterns were altered: the TIE2$^+$ BECs and the HEY1$^+$CD34$^+$DLL4$^+$ BECs lost interactions with PEs, whereas the aSMA$^+$NR2F2$^+$ BECs and the αSMA$^+$DLL4$^+$NR2F2$^+$ BECs were spatially avoiding PEs (Fig 5B). Thus, BEC subsets involved in angiogenesis lost interactions with PEs that are critical for vessel formation, which likely contributes to the angiogenic defects, whereas BEC subsets

organoids from 4 iPSC clones), shown as box plots (median ± IQR). Statistical significance was determined by the Kruskal-Wallis test followed by the Dunn multiple comparisons test. ATACseq, assay for transposase-accessible chromatin sequencing; BVO, blood vessel organoid; CODEX, codetection by indexing; DAR, differentially accessible region; DEG, differentially expressed gene; EC, endothelial cell; EndMT, endothelial-to-mesenchymal transition; GSEA, gene set enrichment analysis; iPSC, induced pluripotent stem cell; RNAseq, RNA sequencing; SSc, systemic sclerosis; SSc_aDU serum, serum from patients with SSc with active digital ulcers; FDR, false discovery rate; PDGFRβ, platelet-derived growth factor receptor beta; COLIV, collagen IV; ICAM, intercellular adhesion molecule; DAPI, 4′,6-diamidino-2-phenylindole; Wnt, Wingless/Integrated; αSMA, alpha-smooth muscle actin; VEGFA, vascular endothelial growth factor A; NES, normalized enrichment score; TGF-β, transforming growth factor beta; TWIST1, twist family bHLH transcription factor 1; ZEB1, zinc finger E-box binding homeobox 1; SNAI1, snail family transcriptional repressor 1; SNAI2, snail family transcriptional repressor 2; FRA2, FOS-related antigen 2; ICAM, intercellular adhesion molecule 1; COL1, collagen type I.

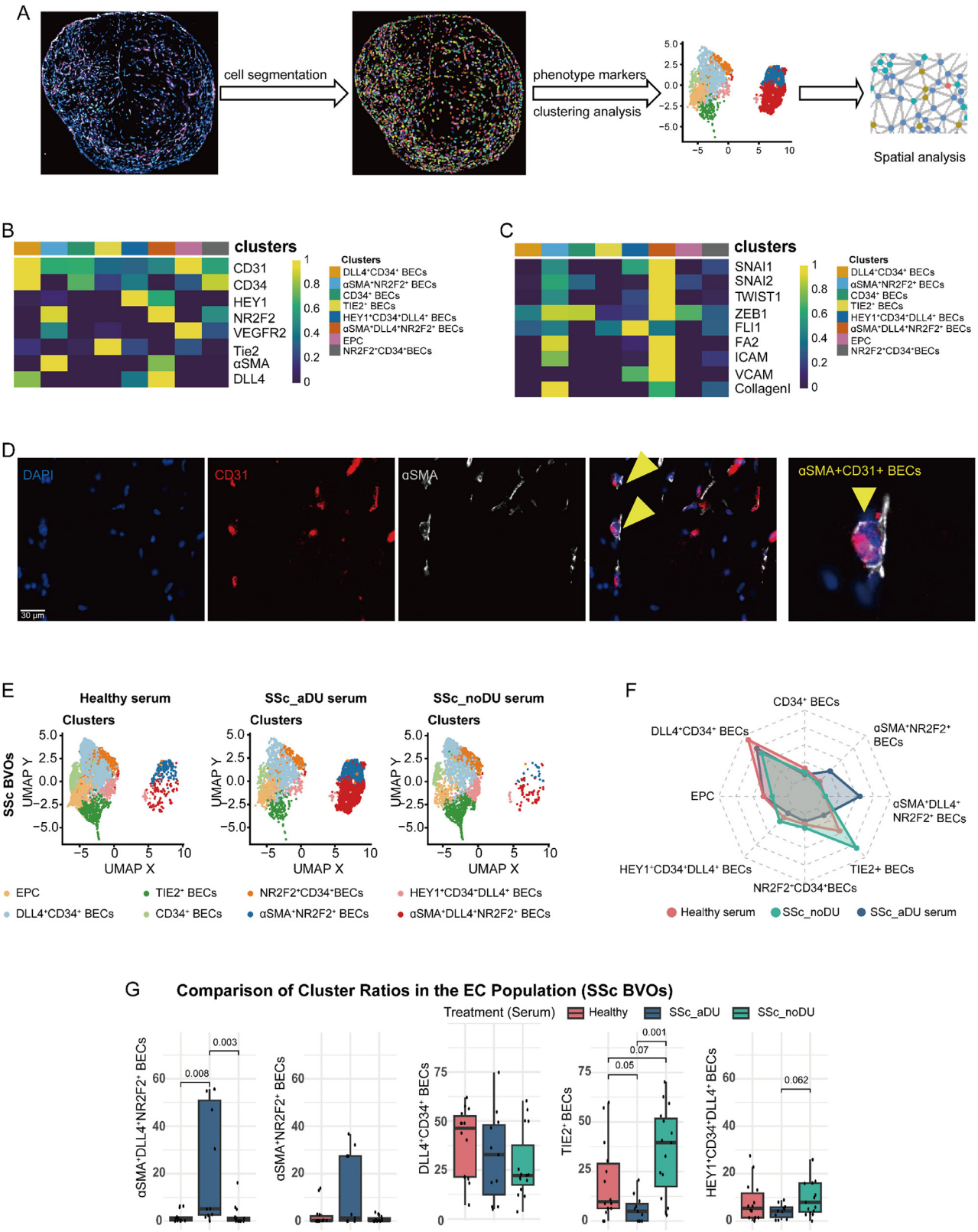

Figure 4. CODEX-based characterisation of endothelial cell subpopulations in SSc BVOs and their shifts upon treatment with SSc serum. (A) Schematic workflow of CODEX single-cell data processing and analysis. Software information for the analyses is provided in Supplementary Table S5. (B, C) Heatmap showing the relative expression levels of endothelial phenotype markers (B) and EndMT markers (C) across BEC subpopulations identified by CODEX analysis. (D) Representative CODEX images of CD31 (red), *α*SMA (grey), and DAPI (blue). Arrowheads indicate *α*SMA + CD31 + BECs. Scale bars = 30 μm. (E) UMAP plots showing the BEC subpopulations in SSc BVOs treated with healthy serum, SSc_aDU serum, or SSc_noDU serum. (F) Radar chart showing the changes in frequencies among BEC subpopulations (from all BECs) upon exposure to healthy serum, SSc_aDU serum, and SSc_noDU serum in SSc BVOs. (G) Changes in frequencies of BEC subpopulations in SSc BVOs exposed to healthy serum, SSc_aDU serum, or SSc_noDU serum ($n \geq 11$ organoids from 4 iPSC clones; samples with <15 total BECs were excluded) shown as box plots (median ± IQR). Statistically significant *P* values (Kruskal-Wallis test followed by Dunn's multiple comparisons test) are included. BEC, blood endothelial cell; BVO, blood vessel organoid; CODEX, codetection by indexing; EC, endothelial cell; EndMT, endothelial-to-mesenchymal transition; EPC, endothelial progenitor cell; iPSC, induced pluripotent stem cell; SSc, systemic sclerosis; SSc_aDU serum, serum from patients with SSc with active digital ulcers; SSc_noDU serum, serum from patients with SSc without active digital ulcers; UMAP, uniform manifold approximation and projection; DAPI, 4′,6-diamidino-2-phenylindole; *α*SMA,

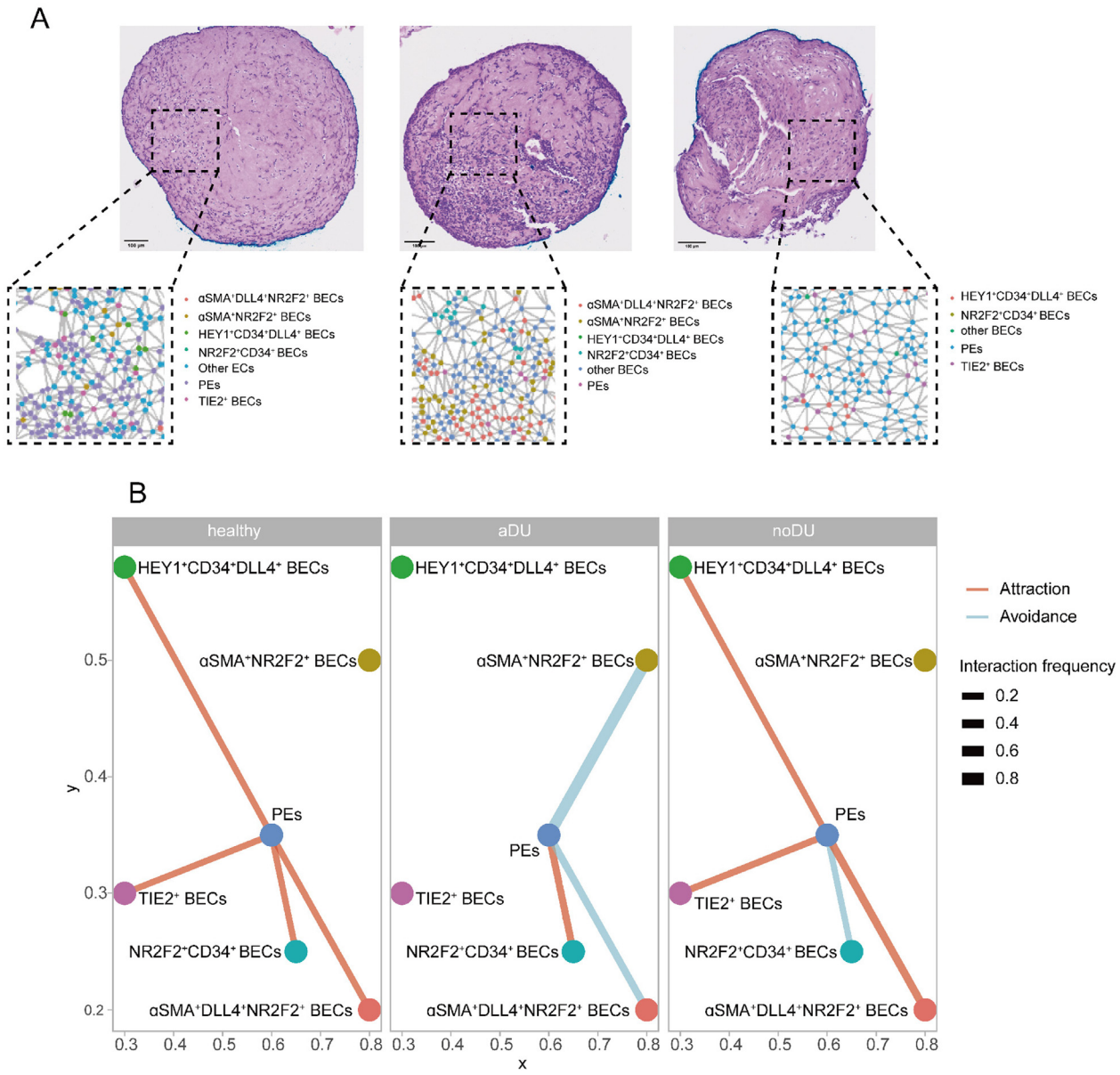

Figure 5. Altered interaction networks between endothelial cell subsets and pericytes in SSc BVOs exposed to SSc serum. (A) Representative histological images (HE stainings) and CODEX-based identification of BEC subpopulations and PEs neighbouring each other (found in close spatial proximity), exposed to healthy serum, SSc_aDU serum, and SSc_noDU serum in SSc BVOs. Scale bars: 100 μm. (B) Interaction network analysis of PEs and BEC subpopulations exposed to healthy serum, SSc_aDU serum, and SSc_noDU serum in SSc BVOs. The width of the lines represents the interaction frequencies, ie, proportion of samples exhibiting statistically significant interactions, with red indicating attraction and blue indicating avoidance. BEC, blood endothelial cell; BVO, blood vessel organoid; CODEX, codetection by indexing; HE, haematoxylin and eosin; PE, pericyte; SSc, systemic sclerosis; SSc_aDU serum, serum from patients with SSc with active digital ulcers; SSc_noDU serum, serum from patients with SSc without active digital ulcers; αSMA, alpha-smooth muscle actin; DLL, Delta-like ligand; HEY1,HES-related family bHLH transcription factor with YRPW motif 1; CD34, cluster of differentiation 34; NR2F2, nuclear receptor subfamily 2 group F member 2; TIE2, tyrosine kinase with immunoglobulin-like and EGF-like domains 2

undergoing EndMT avoided PEs, likely because the mesenchymal phenotype they acquired allowed them to migrate away from vessels. Of note, the interaction network of SSc BVOs exposed to SSc_noDU serum resembled that of SSc BVOs exposed to healthy serum (Fig 5B), highlighting on an additional experimental level that BVOs are specifically reacting to vasoactive mediators from patients with SSc with digital ulcers rather than to factors associated with SSc in general. These results demonstrate that SSc_aDU serum disrupts the physiologic ECs-PEs interaction networks.

SSc serum-induced vasculopathy in SSc BVOs is immunoglobulin G dependent

Since immunoglobulin G (IgG) autoantibodies with direct pathogenic roles in SSc vasculopathy, such as anti-EC antibodies (AECA), antiendothelin receptor type A (anti-ETAR), or antiangiotensin II type 1 receptor (anti-AT1R), were previously described [35–37], we reasoned that IgGs might mediate the deleterious effects of SSc_aDU serum in SSc BVOs. To evaluate this, we treated SSc BVOs with SSc_aDU serum depleted of IgGs

alpha-smooth muscle actin; VEGFR, vascular endothelial growth factor; DLL, Delta-like ligand; HEY1, HES-related family bHLH transcription factor with YRPW motif 1; CD34, cluster of differentiation 34; NR2F2, nuclear receptor subfamily 2 group F member 2; TIE2, tyrosine kinase with immunoglobulin-like and EGF-like domains 2.

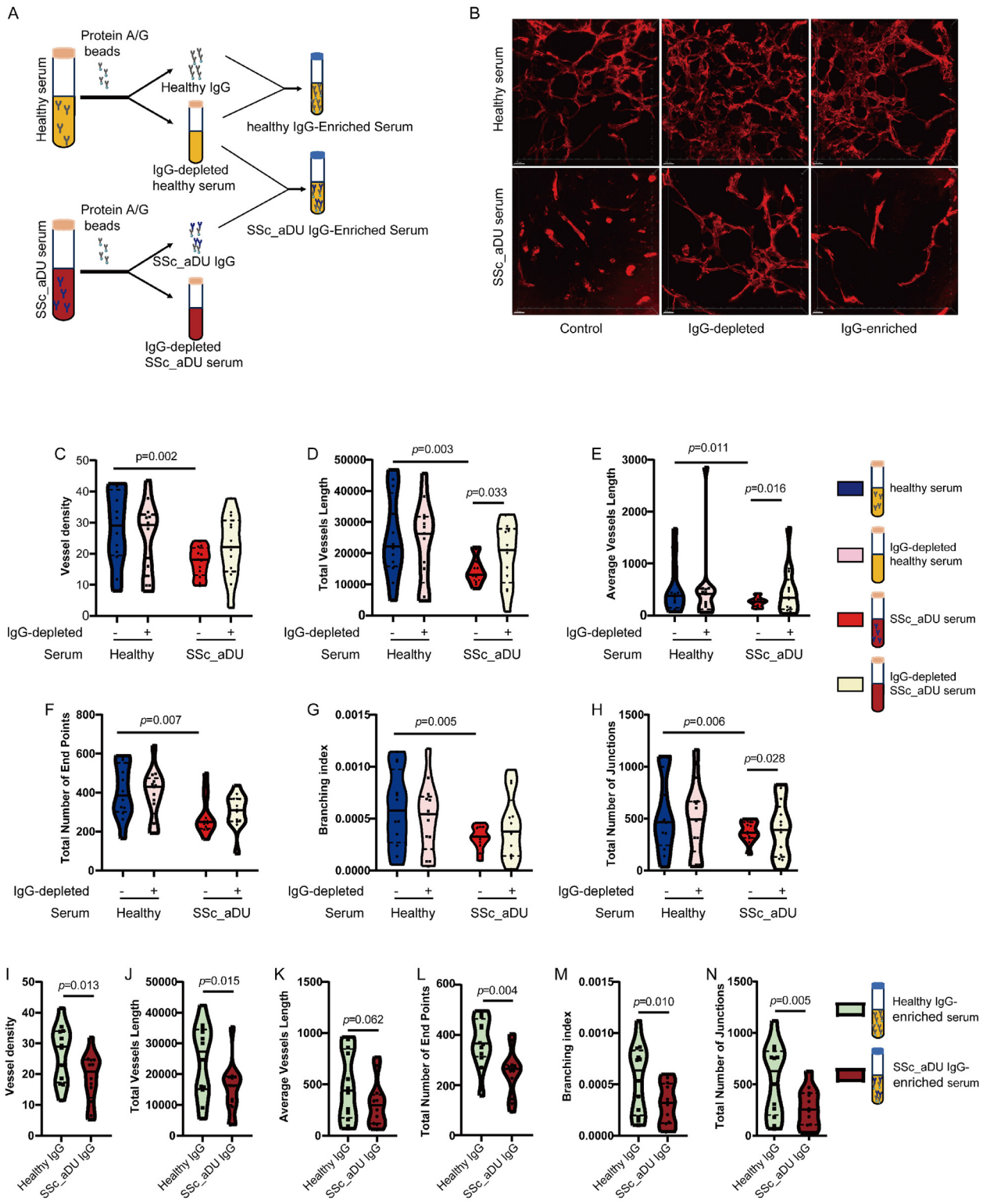

Figure 6. IgG dependency of SSc serum-induced vasculopathy in SSc BVOs. (A) Schematic illustration of depletion of IgG from healthy and SSc_aDU serum, and enrichment of IgG-depleted healthy serum with healthy or SSc_aDU IgG. (B) Representative 3D rendering of confocal images of vascular networks in SSc BVOs treated with complete or IgG-depleted healthy serum or SSc_aDU serum, as well as with SSc_aDU- or healthy IgG-enriched healthy serum (after prior IgG depletion). Endothelial cells forming vessel structures were identified by CD31 marker expression (red). Scale bars, 30 μm. (C-H) Quantitative analysis of vascular parameters of SSc BVOs exposed to complete or IgG-depleted healthy serum or SSc_aDU serum. (I-N) Quantitative analysis of vascular parameters in SSc BVOs treated with healthy IgG-enriched or SSc_aDU IgG-enriched healthy serum (after prior IgG depletion). The analysed vascular parameters include vessel density (C, I), total vessel length (D, J), average vessel length (E, K), total number of endpoints (F, L), branching index (G, M), and total number of junctions (H, N), shown as violin plots. Each condition included 3 different clones with 4 to 5 organoids each. *P* values are from LMMs with serum treatment as a fixed effect and a random intercept for iPSC clone, which accounts for the correlation of organoids derived from the same clone (avoiding pseudoreplication). SSc_aDU serum was pooled from n = 13 donors; active DU was defined as a current open ulcer at sampling (Supplementary Table S2). BVO, blood vessel organoid; IgG, immunoglobulin G; iPSC, induced pluripotent stem cell; LMM, linear mixed-effects model; SSc, systemic sclerosis; SSc_aDU serum, serum from patients with SSc with active digital ulcers; SSc_noDU serum, serum from patients without active digital ulcers; 3D, 3-dimensional.

Table
Serum AECA, anti-ETAR, and anti-AT1R antibodies in patients with SSc_aDU

Antibody	n/N elevated (%)	Median (IQR)	Units
AECA	2/7 (28.6)	1.64 (1.44-2.03)	OD ratio (OD_sample/OD_negative)
ETAR	6/7 (85.7)	12.20 (10.63-15.43)	U/mL
AT1R	3/7 (42.9)	9.01 (7.33-11.09)	U/mL

AECA, antiendothelial cell antibodies; AT1R, angiotensin II type 1 receptor; ETAR, endothelin receptor type A; SSc, systemic sclerosis; SSc_aDU, patients with SSc with active digital ulcers; OD, optical density; OD ratio was calculated as OD_sample/OD_negative.

or with healthy serum enriched in IgGs from SSc_aDU serum (Fig 6A, Supplementary Fig S9).

IgG depletion from SSc_aDU serum partially restored vascular integrity in SSc BVOs, leading to improved network formation and branching, with increased vessel length and number of junctions and numerical increases in vessel density and branching index compared with SSc BVOs exposed to non-IgG-depleted SSc_aDU serum (Fig 6B-H). Enrichment of IgG-depleted healthy serum with IgGs from SSc_aDU serum phenocopied the effects of SSc_aDU serum, and reduced vessel density, vessel length, branching index, and number of junctions in SSc BVOs (Fig 6B,I-N). These findings highlight that IgGs from patients with SSc with severe vasculopathy are central mediators of the effects of SSc_aDU serum in SSc BVOs.

For 7 of the SSc donors that contributed to the pooled SSc_aDU serum, we assessed the presence of AECA, anti-ETAR, and anti-AT1R. AECA positivity was detected in 2 patients (29%), whereas anti-ETAR and anti-AT1R antibody positivity were present in 6 (86%) and 3 (43%) patients, respectively (Table 1), suggesting that these antibodies, and in particular anti-ETAR, might be directly responsible for the antiangiogenic effects of SSc IgGs in SSc BVOs.

SSc BVOs exposed to SSc serum as a model for testing of drugs that target SSc vasculopathy

We next aimed to evaluate the potential of using SSc BVOs exposed to SSc_aDU serum as a platform for evaluating drugs targeting SSc-related vasculopathy. Gene set enrichment analysis of our RNAseq data identified the endothelin pathway as enriched in SSc BVOs upon exposure to SSc_aDU serum (Fig 7A). Given that the endothelin receptor antagonist bosentan (BST) is currently used in clinical practice to prevent the formation of ischaemic fingertip ulcers in SSc [38], we aimed to evaluate whether treatment with BST (Cayman Chemical, Ann Arbor, Michigan, USA) can protect the SSc BVOs from the deleterious effects of SSc_aDU serum. SSc BVOs exposed to SSc_aDU serum and treated with BST had a significantly increased vessel density and total vessel length, numerical differences with increased number of junctions and branching index, and reduced αSMA expression compared with vehicle-treated BVOs (Fig 7B-H,Q,R), thus demonstrating that BST treatment can partially protect against EndMT and vessel damage induced by SSc serum.

We further observed that Notch signalling pathway-associated genes were upregulated in ECs treated with SSc_aDU serum compared with those treated with healthy serum in SSc BVOs (Fig 7I). Aberrant Notch signalling has previously been implicated in diabetes-induced microangiopathy [23]. γ-secretase inhibitors are the most frequently used pharmacological approach to target Notch signalling. Treatment with the γ-secretase inhibitor N-[N-(3,5-difluorophenacetyl)-L-alanyl]-S-phenylglycine t-butyl ester (DAPT; MedChemExpress, Monmouth Junction, New Jersey, USA) protected SSc BVOs from the effects of SSc_aDU serum, with increased vessel density, vessel length, number of junctions, branching index, and reduced αSMA expression (Fig 7J-R).

Taken together, these data demonstrate that SSc BVOs exposed to SSc serum from patients with severe vasculopathy can be used for testing of drugs that target SSc vasculopathy.

DISCUSSION

We provide evidence in the current study that human BVOs can be employed as an *in vitro* model for the study of vascular pathology in SSc and for testing of drugs that target microvasculopathy.

BVOs are differentiated from iPSCs to form ECs assembled as 3D vessels residing on a basement membrane and surrounded by PEs, thus reproducing key features of adult human vessels and being ideally positioned for the study of microvascular responses [16]. We show that BVOs recapitulate important EC populations observed in humans, including LECs, endothelial tip, and stalk cells, involved in angiogenesis, EPCs, ECs committed to an arterial or venous phenotype, and ECs undergoing EndMT. Furthermore, BVOs recapitulate PE subpopulations observed in humans and their interaction with ECs.

BVOs maintain the genetic background of the donor of origin and allow the disentangling of the relative contribution of genetic and environmental factors to a pathologic vascular phenotype. We demonstrate that BVOs generated from SSc donors, thus maintaining the genetic susceptibility of patients with SSc, display features consistent with early stages of vasculopathy observed in patients with SSc, with aberrant angiogenesis and formation of immature vessels. Moreover, these SSc-derived BVOs demonstrate a distinct reaction to external factors compared with healthy BVOs. When exposed to serum from patients with SSc with clinically manifest severe microvasculopathy, they recapitulate typical features of vasculopathy in later stages of SSc, such as loss of small vessels and presence of avascular areas. These phenotypes observed in SSc-derived BVOs resemble the pathologic vascular changes observed in patients with SSc upon evaluation by capillaroscopy as a standard diagnostic tool [7,39]. Notably, SSc serum had only mild effects on angiogenesis in healthy BVOs, suggesting that a susceptible background amplifies the effect. We further demonstrate that the SSc donors carried the *VEGFA* rs2010963 GG genotype, which was previously associated with impaired angiogenesis [24,26,27], whereas the healthy donors carried the CC and CG genotype. This genetic variant might contribute to the higher susceptibility of SSc organoids to the antiangiogenic effects of SSc serum. Although this hypothesis requires validation in future studies, our work nonetheless establishes a methodological framework for future gene variant-specific mechanistic studies of SSc vasculopathy.

We further elucidate the mechanisms leading to angiogenic defects in SSc BVOs exposed to SSc serum. We demonstrate in a multiomics approach that SSc ECs undergo EndMT in the presence of SSc serum, with increased chromatin accessibility assigned to genes related to a mesenchymal phenotype, and decreased accessibility for genes related to an endothelial phenotype, which leads to a corresponding shift in gene expression and pathway activity and to an increased expression of EndMT promoting TFs, markers of myofibroblasts and collagen type 1

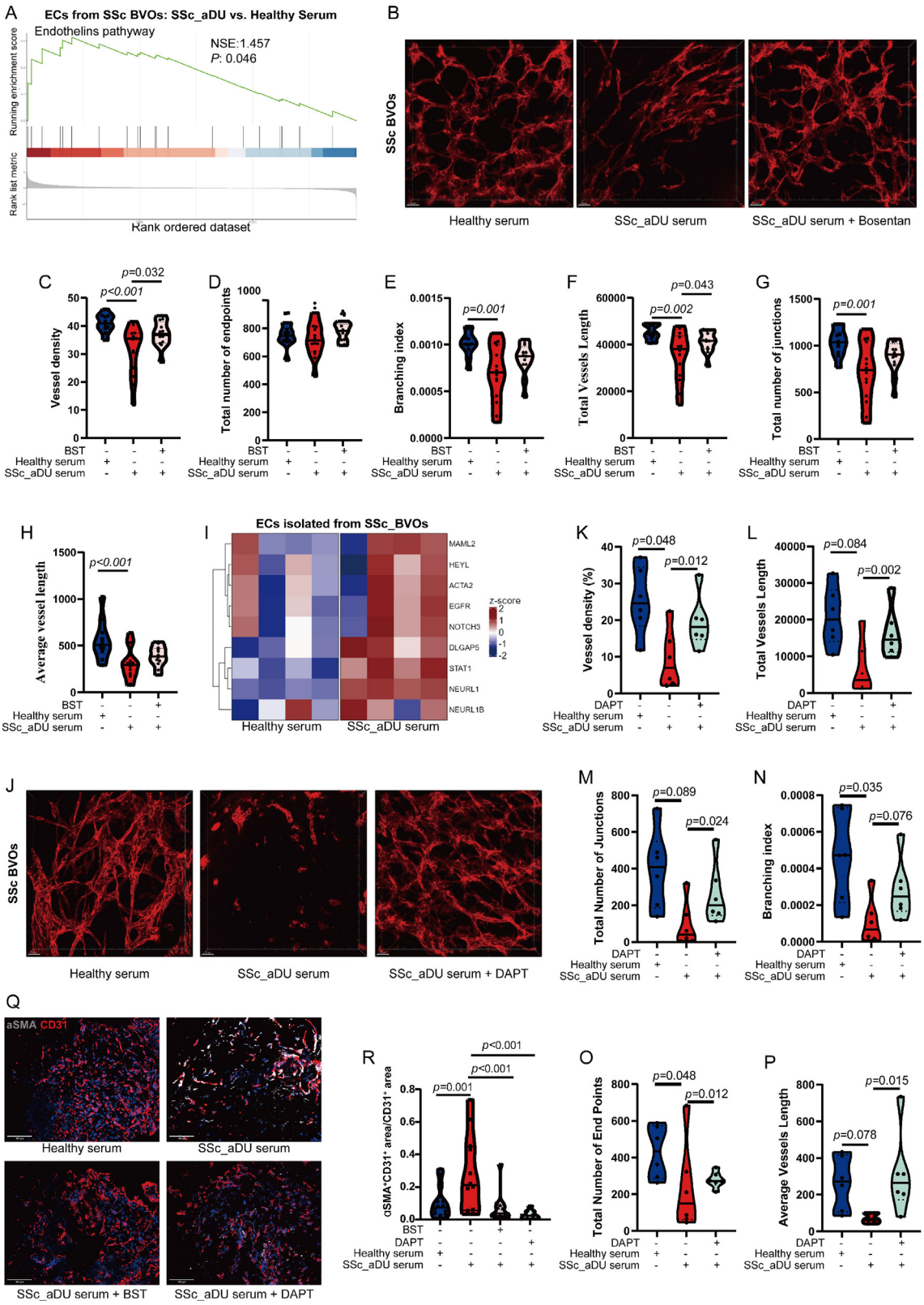

Figure 7. BST and DAPT prevent SSc serum-induced angiogenic defects in SSc BVOs. (A) GSEA enrichment plot of RNAseq data for the term 'Endothelins Pathway' of ECs purified from SSc BVOs exposed to SSc_aDU serum compared with SSc BVOs exposed to healthy serum. (B) Representative 3D rendering of confocal images of vascular networks in SSc BVOs treated with healthy serum, SSc_aDU serum, or BST + SSc_aDU serum for 7 days. CD31 immunostaining (red) was used for identifying vessels. Scale bars, 30 μm. (C-H) Quantitative analysis of vascular parameters in BVOs treated with healthy serum, SSc_aDU serum, or BST + SSc_aDU serum, including vessel density (C), total number of endpoints (D), branching index (E), total vessel length (F), total number of junctions (G), and average vessel length (H). (I) Heatmap of Notch signalling pathway-related genes in ECs purified from SSc BVOs treated with healthy serum or SSc_aDU serum. (J) Representative 3D rendering of confocal images of vascular networks in SSc BVOs treated with healthy serum, SSc_aDU serum, or DAPT + SSc_aDU serum for 7 days. CD31 immunostaining (red) was used for identifying vessels. Scale bars = 30 μm. (K-P) Quantitative analysis of vascular parameters in BVOs treated with healthy serum, SSc_aDU serum, or DAPT + SSc_aDU. (Q) Representative pictures of αSMA-positive endothelial cells in SSc BVOs treated with healthy serum, SSc_aDU serum, BST + SSc_aDU serum, or DAPT + SSc_aDU serum for 7 d. Scale bars, 100 μm. (R) Quantification of the percentage of $\alpha SMA^{+}CD31^{+}$ area from the whole $CD31^{+}$ area in SSc

production. At a single-cell level, this is accompanied by a shift from endothelial stalk or tip cell subsets, as proangiogenic subpopulations, to subpopulations that express high levels of αSMA, collagen type 1 alongside TFs involved in EndMT. Of note, not only ECs but also PEs transition from a PDGFRβ^{hi}αSMA^{-} or CD90^{hi} αSMA^{-} phenotype to an αSMA^{+}SM22^{+} phenotype and thus contribute to the pool of myofibroblasts. EndMT and PE-to-myofibroblast transition have been previously described in the skin of patients with SSc and lungs of patients with SSc-ssociated interstitial lung disease (ILD) [21,31,40,41], thus demonstrating that SSc-BVOs can recapitulate key features of SSc pathology in affected tissues. Not only do the fate transitions of ECs and PEs contribute to the angiogenic defects in SSc BVOs, but also an altered EC-PE interaction network, with, eg, loss of interactions between TIE2^{+} endothelial stalk cells with PEs, interactions that are critical for maturation of newly formed vessels [42,43].

Our data demonstrate that exposure of SSc BVOs to SSc serum induces a dysregulation of a TF network, with reduced expression and/or activity of TFs involved in angiogenesis, such as *ETS1*, *FOXO4*, or *ELK4*, and increased expression and/or activity of TFs involved in EndMT, such as *ZEB1*, *SNAI1*, *SNAI2*, or *TWIST1*. This dysregulation might be the consequence of a sequence of events that involve chromatin remodelling with subsequent changes in mRNA and protein expression to induce transition from an endothelial to a mesenchymal fate.

Thus, exposure of SSc BVOs to SSc serum induces key pathogenic vascular changes observed in patients with SSc that link vasculopathy with tissue fibrosis. BVOs might, thus, be used to study not only vasculopathy but also the transition and the relative contribution of vasculopathy to tissue fibrosis. Furthermore, our data suggest that ECs from SSc BVOs exposed to SSc serum upregulate the adhesion molecules ICAM and might promote leukocyte migration and activation. A previous study demonstrated that interleukin-1 beta (IL-1β)-activated ECs can trigger alternative activation of macrophages, which subsequently induce fibroblast activation [44]. Macrophages could be included in BVOs to study and potentially interfere with the crosstalk between ECs and macrophages.

The inhibitory effects of serum from patients with SSc with severe SSc vasculopathy are at least in part mediated by IgG autoantibodies, since depletion of IgGs prevents these effects, whereas enrichment of IgG-depleted healthy serum with SSc IgGs phenocopies the effects of complete SSc serum. Several autoantibodies present in patients with SSc could potentially mediate these effects. Patients with SSc with digital ulcers exhibit higher levels of AECA in serum compared with those without digital ulcers [37,45], and AECA has been identified as a marker of vascular damage [46]. Furthermore, anti-AT1R and anti-ETAR antibody-positive IgGs from SSc sera were previously shown to induce changes in the phenotype of ECs [36]. We show that the sera of most SSc donors with vasculopathic manifestations used in our experiments were positive for anti-AT1R, and a high percentage were positive for anti-ETAR or AECA, suggesting a potential role of these autoantibodies, which remains to be validated in future studies.

However, pathogenic autoantibodies might not be the only mechanism responsible for the deleterious effects of SSc serum. Matrix metalloproteinase-12 (MMP-12)-dependent urokinase plasminogen activator receptor domain 1 (uPAR-D1) cleavage, eg, was previously shown to mediate the induction of EndMT by SSc serum [47].

We further demonstrate that treatment with the endothelin-1 (ET-1) antagonist BST or with the γ-secretase inhibitor DAPT prevents microvascular changes and EndMT induced by SSc serum in SSc BVOs. BST was previously shown to prevent angiogenic defects and EndMT in ECs cocultured with SSc fibroblasts [48], and is currently in clinical use in SSc for the prevention of recurring digital ulcers [49]. The efficacy of BST in BVOs, thus, serves as proof of concept that BVOs respond to well-established drugs that target SSc vasculopathy. Notch signalling was previously shown to be upregulated in SSc [28,50], and 1 of the αSMA^{+} EC subsets defined by our CODEX approach expresses high levels of the Notch ligand DLL4. The efficacy of DAPT in ameliorating SSc serum-induced vasculopathy in SSc BVOs provides evidence that aberrant Notch signalling is involved in mediating angiogenic defects and EndMT in SSc. Our data could, thus, stimulate follow-up studies with γ-secretase inhibitors for the treatment of SSc vasculopathy.

Our study has limitations. The main experiments were performed with iPSCs from 2 SSc donors (both male) and 2 healthy donors, with 2 clones per donor. We therefore prioritised in-depth analyses of SSc-serum effects rather than expanding the number of iPSC lines, and the limited number of SSc iPSC donors limits generalisability and precludes assessment of interindividual variability. However, the small sample size applies only to the iPSC donors; in the serum treatment experiments, we used pooled sera from 13 patients with SSc with active digital ulcers (defined as current open ulcers with tissue loss at the time of serum collection) and 5 patients without active digital ulcers. The iPSC donors from healthy donors and patients with SSc were not gender matched. However, further comparison of healthy female and male BVOs showed comparable vessel density and architecture between male- and female-derived healthy organoids, suggesting that, within our system, baseline sex-related effects on angiogenesis are limited, although sex-specific interactions with SSc serum cannot be excluded. In this study, we pooled sera from multiple donors for the serum treatment experiments, which precludes stratified analyses according to donor-specific characteristics other than the presence of active digital ulcers. This design, however, attenuates the influence of single-donor outliers and idiosyncratic exposures of the organoids.

In summary, we characterised SSc-BVOs as a novel human model system to study SSc-associated vasculopathy. We provide evidence that genetic predisposition and circulating mediators, such as autoantibodies from SSc serum, synergise to produce a broader range of SSc-like vascular changes in this system such as upregulated EndMT, PE-to-mesenchymal transition, and loss of ECs-PEs interactions in BVOs, which result in dysfunctional angiogenesis and perivascular fibrosis. Exposure of SSc-BVOs to SSc serum triggers changes on epigenetic, mRNA and protein levels to downregulate proangiogenic pathways and activate

BVOs treated with healthy serum, SSc_aDU serum, DAPT + SSc_aDU serum, or BST + SSc_aDU serum. Each condition included 4 iPSC clones with 1 to 4 organoids each. *P* values are from LMMs with serum/BST/DAPT treatment as a fixed effect and a random intercept for iPSC clone, which accounts for the correlation of organoids derived from the same clone (avoiding pseudoreplication). SSc_aDU serum was pooled from n = 13 donors; active DU was defined as a current open ulcer at sampling (Supplementary Table S2). ATACseq, assay for transposase-accessible chromatin sequencing; BST, bosentan; BVO, blood vessel organoid; CODEX, codetection by indexing; EC, endothelial cell; GSEA, gene set enrichment analysis; iPSC, induced pluripotent stem cell; LMM, linear mixed-effects model; RNAseq, RNA sequencing; SSc, systemic sclerosis; SSc_aDU serum, serum from patients with SSc with active digital ulcers; 3D, 3-dimensional; DAPT, N-[N-(3,5-difluorophenacetyl)-L-alanyl]-S-phenylglycine t-butyl ester; αSMA, alpha-smooth muscle actinBST, bosentan

EndMT programmes. We also show that SSc-BVOs can serve as a preclinical model system to evaluate the effects of drug candidates on SSc microvasculopathy and use this model to provide the first evidence for potential therapeutic effects of γ-secretase inhibition on SSc vasculopathy.

Acknowledgements

We thank Sonja Plötz, Michaela Farrell, Christoph Liebel, Philipp Steinbrecher, Lukas Sokolowski, and Wolfgang Espach for excellent technical assistance. We further thank Figdraw for their assistance in creating symbols. Fluorescence microscopy was performed at the Advanced Light Microscopy Core Facility (Ad-Light), Medical Faculty of the Heinrich Heine University, Düsseldorf. Our analysis was supported by a de.NBI Cloud project (YNL) within the German Network for Bioinformatics Infrastructure (de.NBI) and ELIXIR-DE (Forschungszentrum Jülich and W-de.NBI-001, W-de.NBI-004, W-de.NBI-008, W-de.NBI-010, W-de.NBI-013, W-de.NBI-014, W-de.NBI-016, and W-de.NBI-022).

Contributors

YX, JHWD, and A-EM designed the study. YX, XH, LZ, Y-NL, BG, SK, A-HG, TF, P-MB, PT, and A-EM were involved in the acquisition and analysis of data. All authors were involved in the interpretation of data. MR, FM, JA, and JW provided essential samples. All authors were involved in manuscript preparation and proofreading.

Funding

Confocal spinning disc microscopy was enabled on a Zeiss Spinning Disc Axio Observer Z1, funded by Deutsche Forschungsgemeinschaft (DFG, German Research Foundation)—project 248122450.

The project was supported by the following grants: Grants DI 1537/17-1, DI 1537/20-1, DI 1537/22-1, DI 1537/23-1, DI 1537/27-1, and DI 1537/28-1 of the German Research Foundation (JHWD), MA 9219/2-1 of the German Research Foundation (AEM), 493659010 of the German Research Foundation, SFB CRC1181 (project C01) of the German Research Foundation, grants 2021_EKEA.03 (AEM) and 2022_EKMS.02 (AEM) of the Else-Kröner-Fresenius-Foundation, The Edith Busch and World Scleroderma Foundation Research Grant Programme 2022-2023 (AEM), the German Federal Ministry of Education and Research (BMBF), MASCARA program, TP 2 (01EC1903A), ACS_iIMMUNE (01EO2105 to MR), the Research Committee of the Medical Faculty of the Heinrich-Heine University Düsseldorf (Forschungskommission; ID 2022-18, ID 2023-33 and ID 2023-31 to AHG, AEM, and JHWD, respectively), an unrestricted research grant from the Hiller-Foundation (JHWD), and a Career Support Award of Medicine of the Ernst Jung Foundation (JHWD).

Competing interests

A-HG received lecture fees from Boehringer Ingelheim. JHWD has consultancy relationships with Active Biotech, Anamar, ARXX, AstraZeneca, Bayer Pharma, Boehringer Ingelheim, Callidatas, Calluna, Galapagos, GSK, Janssen, Kyverna, Novartis, Pfizer, Quell Therapeutics, and UCB. JHWD has received research funding from Anamar, ARXX, BMS, Boehringer Ingelheim, Cantargia, Celgene, CSL Behring, Exo Therapeutics, Galapagos, GSK, Incyte, Inventiva, Kiniksa, Kyverna, Lassen Therapeutics, Mestag, Sanofi-Aventis, SpicaTx, RedX, UCB, and ZenasBio. JHWD is the CEO of 4D Science and the scientific lead of FibroCure. All other authors declare no competing interests. All other authors declare they have no competing interests.

Patient consent for publication

Not applicable.

Ethics approval

All donors provided informed consent for participation in the study. Fibroblast isolation and reprogramming to iPSC, as well as the experiments performed with the iPSC were approved by the Ethical Committee of the University of Erlangen-Nürnberg and the Ethical Commit-tee of the University of Düsseldorf (approval numbers: 21-485-Bp, 98_18 B, 30_19B (Erlan-gen) and 2022-2158 (Düsseldorf)).

Provenance and peer review

Not commissioned; externally peer reviewed

Data availability statement

RNAseq and ATACseq data generated in this study have been deposited in the NCBI Gene Expression Omnibus (GEO) under accession number GSE307380. Any further information required to reanalyse the data reported in this paper should be directed to, and will be provided by the lead contact: Alexandru-Emil Matei (alexandru-emil.matei@med.uni-duesseldorf.de).

Supplementary materials

Supplementary material associated with this article can be found in the online version at doi:10.1016/j.ard.2026.02.021.

Orcid

Alexandru-Emil Matei: http://orcid.org/0000-0003-1248-3145

REFERENCES

[1] Denton CP, Khanna D. Systemic sclerosis. Lancet 2017;390:1685–99. doi: 10.1016/S0140-6736(17)30933-9.
[2] Distler JHW, Györfi A-H, Ramanujam M, Whitfield ML, Königshoff M, Lafyatis R. Shared and distinct mechanisms of fibrosis. Nat Rev Rheumatol 2019;15:705–30. doi: 10.1038/s41584-019-0322-7.
[3] Kawaguchi Y, Kuwana M. Pathogenesis of vasculopathy in systemic sclerosis and its contribution to fibrosis. Curr Opin Rheumatol 2023;35:309–16. doi: 10.1097/BOR.0000000000000959.
[4] Distler JHW, Kuwana M, Assassi S, Denton CP. Emerging therapies for the treatment of systemic sclerosis. Nat Rev Rheumatol 2025;21:612–25. doi: 10.1038/s41584-025-01294-x.
[5] Matucci-Cerinic M, Kahaleh B, Wigley FM. Review: evidence that systemic sclerosis is a vascular disease. Arthritis Rheum 2013;65:1953–62. doi: 10.1002/art.37988.
[6] Di Benedetto P, Ruscitti P, Liakouli V, Cipriani P, Giacomelli R. The vessels contribute to fibrosis in systemic sclerosis. Isr Med Assoc J 2019;21:471–4.
[7] Cutolo M, Sulli A, Pizzorni C, Accardo S. Nailfold videocapillaroscopy assessment of microvascular damage in systemic sclerosis. J Rheumatol 2000; 27:155–60.
[8] Liakouli V, Cipriani P, Marrelli A, Alvaro S, Ruscitti P, Giacomelli R. Angiogenic cytokines and growth factors in systemic sclerosis. Autoimmun Rev 2011;10:590–4. doi: 10.1016/j.autrev.2011.04.019.
[9] Manetti M, Guiducci S, Romano E, Ceccarelli C, Bellando-Randone S, Conforti ML, et al. Overexpression of VEGF165b, an inhibitory splice variant of

vascular endothelial growth factor, leads to insufficient angiogenesis in patients with systemic sclerosis. Circ Res 2011;109:e14–26. doi: 10.1161/CIRCRESAHA.111.242057.
[10] Moritz F, Schniering J, Distler JHW, Gay RE, Gay S, Distler O, et al. Tie2 as a novel key factor of microangiopathy in systemic sclerosis. Arthritis Res Ther 2017;19:105. doi: 10.1186/s13075-017-1304-2.
[11] Manetti M, Allanore Y, Revillod L, Fatini C, Guiducci S, Cuomo G, et al. A genetic variation located in the promoter region of the UPAR (CD87) gene is associated with the vascular complications of systemic sclerosis. Arthritis Rheum 2011;63:247–56. doi: 10.1002/art.30101.
[12] Pu W, Wu W, Liu Q, Ma Y, Tu W, Zuo X, et al. Exome-wide association analysis suggests LRP2BP as a susceptibility gene for endothelial injury in systemic sclerosis in the Han Chinese population. J Invest Dermatol 2021;141:1254–63 e6. doi: 10.1016/j.jid.2020.07.039.
[13] López-Isac E, Acosta-Herrera M, Kerick M, Assassi S, Satpathy AT, Granja J, et al. GWAS for systemic sclerosis identifies multiple risk loci and highlights fibrotic and vasculopathy pathways. Nat Commun 2019;10:4955. doi: 10.1038/s41467-019-12760-y.
[14] Maurer B, Distler JHW, Distler O. The Fra-2 transgenic mouse model of systemic sclerosis. Vascul Pharmacol 2013;58:194–201. doi: 10.1016/j.vph.2012.12.001.
[15] Wimmer RA, Leopoldi A, Aichinger M, Kerjaschki D, Penninger JM. Generation of blood vessel organoids from human pluripotent stem cells. Nat Protoc 2019;14:3082–100. doi: 10.1038/s41596-019-0213-z.
[16] Wimmer RA, Leopoldi A, Aichinger M, Wick N, Hantusch B, Novatchkova M, et al. Human blood vessel organoids as a model of diabetic vasculopathy. Nature 2019;565:505–10. doi: 10.1038/s41586-018-0858-8.
[17] Zudaire E, Gambardella L, Kurcz C, Vermeren S. A computational tool for quantitative analysis of vascular networks. PLoS One 2011;6:e27385. doi: 10.1371/journal.pone.0027385.
[18] Bumgarner JR, Nelson RJ. Open-source analysis and visualization of segmented vasculature datasets with VesselVio. Cell Rep Methods 2022;2:100189. doi: 10.1016/j.crmeth.2022.100189.
[19] Manetti M, Guiducci S, Ibba-Manneschi L, Matucci-Cerinic M. Mechanisms in the loss of capillaries in systemic sclerosis: angiogenesis versus vasculogenesis. J Cell Mol Med 2010;14:1241–54. doi: 10.1111/j.1582-4934.2010.01027.x.
[20] Matucci-Cerinic M, Manetti M, Bruni C, Chora I, Bellando-Randone S, Lepri G, et al. The "myth" of loss of angiogenesis in systemic sclerosis: a pivotal early pathogenetic process or just a late unavoidable event? Arthritis Res Ther 2017;19:162. doi: 10.1186/s13075-017-1370-5.
[21] Romano E, Rosa I, Fioretto BS, Manetti M. Recent insights into cellular and molecular mechanisms of defective angiogenesis in systemic sclerosis. Biomedicines 2024;12:1331. doi: 10.3390/biomedicines12061331.
[22] Cai L, Chen Y, Shan C, Zhao Q, Luo J, Li X, et al. A case-control study of the interaction of the eNOS gene polymorphisms rs1799983 and rs1800780 with acute coronary syndrome (ACS) risk factors. BMC Cardiovasc Disord 2025;25:446. doi: 10.1186/s12872-025-04891-6.
[23] Wang Y, Zheng Y, Zhang W, Yu H, Lou K, Zhang Y, et al. Polymorphisms of KDR gene are associated with coronary heart disease. J Am Coll Cardiol 2007;50:760–7. doi: 10.1016/j.jacc.2007.04.074.
[24] Lambrechts D, Storkebaum E, Morimoto M, Del-Favero J, Desmet F, Marklund SL, et al. VEGF is a modifier of amyotrophic lateral sclerosis in mice and humans and protects motoneurons against ischemic death. Nat Genet 2003;34:383–94. doi: 10.1038/ng1211.
[25] Cui L, Jing S, Wang X, Zong Q, Li X, Jiao C, et al. Rs5498 polymorphism may be a risk factor for coronary heart disease in Chinese population: evidence from a meta-analysis involving 5537 subjects. Int J Clin Exp Med 2015;8:17461–70.
[26] Awata T, Inoue K, Kurihara S, Ohkubo T, Watanabe M, Inukai K, et al. A common polymorphism in the 5'-untranslated region of the VEGF gene is associated with diabetic retinopathy in type 2 diabetes. Diabetes 2002;51:1635–9. doi: 10.2337/diabetes.51.5.1635.
[27] Xie J, Yi L, Xu Z-F, Mo XM, Hu YL, Wang DJ, et al. VEGF C-634G polymorphism is associated with protection from isolated ventricular septal defect: case-control and TDT studies. Eur J Hum Genet 2007;15:1246–51. doi: 10.1038/sj.ejhg.5201890.
[28] Huang M, Tabib T, Khanna D, Assassi S, Domsic R, Lafyatis R. Single-cell transcriptomes and chromatin accessibility of endothelial cells unravel transcription factors associated with dysregulated angiogenesis in systemic sclerosis. Ann Rheum Dis 2024;83:1335–44. doi: 10.1136/ard-2023-225415.
[29] Rius Rigau A, Li Y-N, Matei A-E, Györfi AH, Bruch PM, Koziel S, et al. Characterization of vascular niche in systemic sclerosis by spatial proteomics. Circ Res 2024;134:875–91. doi: 10.1161/CIRCRESAHA.123.323299.
[30] Robinson WH, Younis S, Love ZZ, Steinman L, Lanz TV. Epstein-Barr virus as a potentiator of autoimmune diseases. Nat Rev Rheumatol 2024;20:729–40. doi: 10.1038/s41584-024-01167-9.
[31] Di Benedetto P, Ruscitti P, Berardicurti O, Vomero M, Navarini L, Dolo V, et al. Endothelial-to-mesenchymal transition in systemic sclerosis. Clin Exp Immunol 2021;205:12–27. doi: 10.1111/cei.13599.
[32] Patnaik E, Lyons M, Tran K, Pattanaik D. Endothelial dysfunction in systemic sclerosis. Int J Mol Sci 2023;24:14385. doi: 10.3390/ijms241814385.
[33] Teichert M, Milde L, Holm A, Stanicek L, Gengenbacher N, Savant S, et al. Pericyte-expressed Tie2 controls angiogenesis and vessel maturation. Nat Commun 2017;8:16106. doi: 10.1038/ncomms16106.
[34] Aguilera KY, Brekken RA. Recruitment and retention: factors that affect pericyte migration. Cell Mol Life Sci 2014;71:299–309. doi: 10.1007/s00018-013-1432-z.
[35] Ahmed SS, Tan FK, Arnett FC, Jin L, Geng YJ. Induction of apoptosis and fibrillin 1 expression in human dermal endothelial cells by scleroderma sera containing anti-endothelial cell antibodies. Arthritis Rheum 2006;54:2250–62. doi: 10.1002/art.21952.
[36] Kill A, Tabeling C, Undeutsch R, Kühl AA, Günther J, Radic M, et al. Autoantibodies to angiotensin and endothelin receptors in systemic sclerosis induce cellular and systemic events associated with disease pathogenesis. Arthritis Res Ther 2014;16:R29. doi: 10.1186/ar4457.
[37] Kayser C, Fritzler MJ. Autoantibodies in systemic sclerosis: unanswered questions. Front Immunol 2015;6:167. doi: 10.3389/fimmu.2015.00167.
[38] Sfikakis PP, Papamichael C, Stamatelopoulos KS, Tousoulis D, Fragiadaki KG, Katsichti P, et al. Improvement of vascular endothelial function using the oral endothelin receptor antagonist bosentan in patients with systemic sclerosis. Arthritis Rheum 2007;56:1985–93. doi: 10.1002/art.22634.
[39] Lambova SN, Müller-Ladner U. Nailfold capillaroscopy in systemic sclerosis - state of the art: the evolving knowledge about capillaroscopic abnormalities in systemic sclerosis. J Scleroderma Relat Disord 2019;4:200–11. doi: 10.1177/2397198319833486.
[40] Cipriani P, Di Benedetto P, Ruscitti P, Liakouli V, Berardicurti O, Carubbi F, et al. Perivascular cells in diffuse cutaneous systemic sclerosis overexpress activated ADAM12 and are involved in myofibroblast transdifferentiation and development of fibrosis. J Rheumatol 2016;43:1340–9. doi: 10.3899/jrheum.150996.
[41] Cipriani P, Di Benedetto P, Ruscitti P, Capece D, Zazzeroni F, Liakouli V, et al. The endothelial-mesenchymal transition in systemic sclerosis is induced by endothelin-1 and transforming growth factor-β and may be blocked by macitentan, a dual endothelin-1 receptor antagonist. J Rheumatol 2015;42:1808–16. doi: 10.3899/jrheum.150088.
[42] van Splunder H, Villacampa P, Martínez-Romero A, Graupera M. Pericytes in the disease spotlight. Trends Cell Biol 2024;34:58–71. doi: 10.1016/j.tcb.2023.06.001.
[43] Savant S, La Porta S, Budnik A, Busch K, Hu J, Tisch N, et al. The orphan receptor Tie1 controls angiogenesis and vascular remodeling by differentially regulating Tie2 in tip and stalk cells. Cell Rep 2015;12:1761–73. doi: 10.1016/j.celrep.2015.08.024.
[44] Laurent P, Lapoirie J, Leleu D, Levionnois E, Grenier C, Jurado-Mestre B, et al. Interleukin-1β-activated microvascular endothelial cells promote DC-SIGN-positive alternatively activated macrophages as a mechanism of skin fibrosis in systemic sclerosis. Arthritis Rheumatol 2022;74:1013–26. doi: 10.1002/art.42061.
[45] Sunderkötter C, Herrgott I, Brückner C, Moinzadeh P, Pfeiffer C, Gerss J, et al. Comparison of patients with and without digital ulcers in systemic sclerosis: detection of possible risk factors. Br J Dermatol 2009;160:835–43. doi: 10.1111/j.1365-2133.2008.09004.x.
[46] Abraham DJ, Krieg T, Distler J, Distler O. Overview of pathogenesis of systemic sclerosis. Rheumatology (Oxford) 2009;48(Suppl 3):iii3–7. doi: 10.1093/rheumatology/ken481.
[47] Manetti M, Romano E, Rosa I, Guiducci S, Bellando-Randone S, De Paulis A, et al. Endothelial-to-mesenchymal transition contributes to endothelial dysfunction and dermal fibrosis in systemic sclerosis. Ann Rheum Dis 2017;76:924–34. doi: 10.1136/annrheumdis-2016-210229.
[48] Corallo C, Cutolo M, Kahaleh B, Pecetti G, Montella A, Chirico C, et al. Bosentan and macitentan prevent the endothelial-to-mesenchymal transition (EndoMT) in systemic sclerosis: in vitro study. Arthritis Res Ther 2016;18:228. doi: 10.1186/s13075-016-1122-y.
[49] Matucci-Cerinic M, Denton CP, Furst DE, Mayes MD, Hsu VM, Carpentier P, et al. Bosentan treatment of digital ulcers related to systemic sclerosis: results from the RAPIDS-2 randomised, double-blind, placebo-controlled trial. Ann Rheum Dis 2011;70:32–8. doi: 10.1136/ard.2010.130658.
[50] Dees C, Zerr P, Tomcik M, Beyer C, Horn A, Akhmetshina A, et al. Inhibition of Notch signaling prevents experimental fibrosis and induces regression of established fibrosis. Arthritis Rheum 2011;63:1396–404. doi: 10.1002/art.30254.